New World hummingbirds and Australian honeyeaters[9].

Seven out of eight captured sunbirds were carrying pollinaria or partial pollinaria on their tongues, with up to four corpusculi attached at a time (median number of corpusculi per bird, 2; median number of pollen sacs per bird, 0.5). The frequent presence of corpusculi with only one or neither of their two pollen sacs attached suggests that pollen sacs were transferred successfully to other flowers.

As expected from the high levels of flower visitation, a large proportion (54%) of flowers were found to be pollinated ($n = 48$). Three times more pollen sacs were removed (2.90 ± 2.74 per flower) than reinserted (0.96 ± 1.01; $n = 48$), indicating substantial losses during transfer. Seed pod production is high in plants exposed to sunbirds, whereas bagged (pollinator excluded) flowers set no seeds ($n = 119$).

A captive sunbird was used to test whether sunbirds successfully transfer pollen sacs to the intricate pollen-receiving mechanism (Fig. 1d). I exposed 37 virgin *M. sagittatum* flowers to the bird for a period of two minutes per flower. There were no insects in the cage. Dissection showed that the 37 experimental flowers received 39 pollen sacs, indicating that sunbirds effectively both collect and deliver pollen sacs.

Plants adapted for pollen transfer on bird tongues are characterized by having: (1) tough and streamlined pollinaria with a mechanical clip; (2) morphology that excludes insects; (3) reddish coloration; (4) copious, dilute nectar; and (5) no scent. Applying these criteria to the rest of the genus *Microloma*[5], I predict that six of the nine remaining species are pollinated in the manner described here. Outside Africa, many members of the large southeast Asian genus *Dischidia*[10] are among other plants that may be adapted for pollen transfer on the tongues of birds. Anecdotal accounts of sunbirds, hummingbirds and honeyeaters visiting the flowers of several genera of Asclepiadaceae[2] beg investigation.

Anton Pauw
Department of Botany,
University of Cape Town,
Private Bag, Rondebosch 7701,
Cape Town, South Africa
e-mail: pauw@botzoo.uct.ac.za

1. Kunze, H. *Plant Syst. Evol.* **176,** 227–253 (1991).
2. Ollerton, J. & Liede, S. *Biol. J. Linn. Soc.* **62,** 593–610 (1997).
3. Faegri, K. & van der Pijl, L. *The Principles of Pollination Ecology.* (Pergamon, Oxford, 1979).
4. Vogel, S. *Bot. Stud.* **1,** 1–338 (1954).
5. Bruyns, P. & Linder, H. P. *Bot. Jahrb. Syst.* **112,** 453–527 (1991).
6. Wanntorp, H. E. *Opera Bot.* **98,** 1–69 (1988).
7. Marloth, R. *The Flora of South Africa, Vol. 3* (Darter, Cape Town, 1932).
8. Kearns, C. A. & Inouye, D. W. *Techniques for Pollination Biologists* (Univ. Press of Colorado, Niwot, 1993).
9. Paton, D. C. & Collins, B. G. *Aust. J. Ecol.* **14,** 473–506 (1989).
10. Rintz, R. E. *Blumea* **26,** 81–126 (1980).

A proxy index of ENSO teleconnections

Variations in central and eastern equatorial sea surface temperatures are linked to extra-tropical climate changes by atmospheric heat and moisture fluxes in so-called 'teleconnection' patterns[1,2]. Estimates of sea surface temperature (SST) anomaly may be derived from the isotopic composition and minor-element chemistry of aragonite formed by annually banded reef corals. Here we reconstruct anomalies in central equatorial Pacific SSTs for 1938–93 from the stable oxygen isotope (δ^{18}O) composition of a coral collected at Kiritimati (Christmas) Island, Republic of Kiribati (157.3° W, 2° N). We recover not only the regional anomaly in SST, but also extra-tropical climate information in climatically teleconnected regions.

Interannual variability in the δ^{18}O composition of aragonite is a function of the temperature of the sea surface in which the coral secretes its skeleton[3]. This variability in coral δ^{18}O also records any changes in the δ^{18}O of sea water, which may be significant in some oceanographic settings[4].

The strontium-to-calcium (Sr/Ca) ratio in corals is also a function of SST, but seawater Sr/Ca variability is minimal[5,6]. Application of these two proxies in tandem has been used to estimate both seawater δ^{18}O and SST anomalies during the 1982–83 El Niño–Southern Oscillation (ENSO) event from measurements made on Great Barrier Reef corals[7]. In principle, paired Sr/Ca and δ^{18}O data from a series of temporally overlapping coral cores may yield proxy estimates of SST and seawater δ^{18}O variability extending well into the pre-instrumental period.

At Kiritimati, seasonal SST varies by ≤ 1.2 °C, whereas ENSO-induced SST anomalies of ± 3 °C reflect changes in wind stress and associated equatorial upwelling[8]. Thus, Kiritimati is an ideal location at which to monitor the thermal oceanographic signal associated with the full ENSO cycle. We measured δ^{18}O and carbon isotopic (δ^{13}C) composition in a core from a living coral, collected in March 1994, at intervals of 0.5 mm along the maximal growth axis of the coral.

We used the δ^{13}C record to construct an age model for analysis of the δ^{18}O record over time, on the basis of observations of the dependence of δ^{13}C levels in coralline aragonite on coralline reproductive

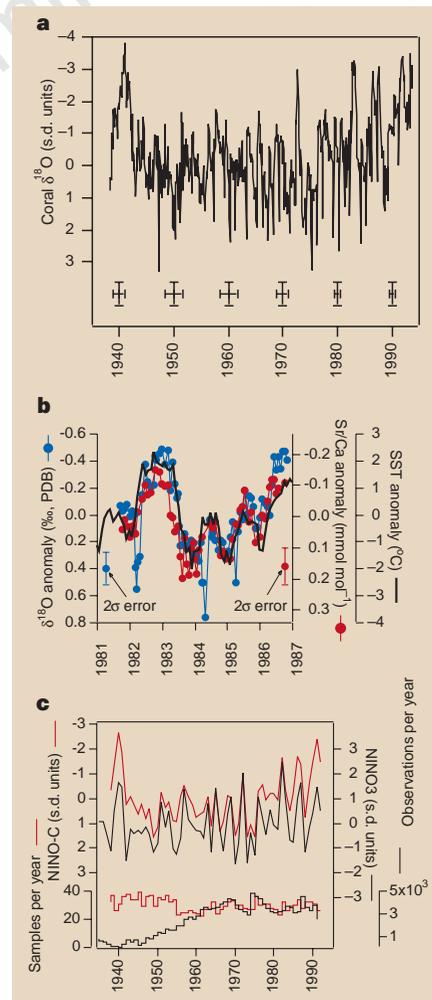**Figure 1** Kiritimati coral proxy data. **a,** Kiritimati coral δ^{18}O time series normalized to the 1951–80 mean and standard deviation of the data. The δ^{18}O scale has been reversed for direct comparison with SST anomalies (**b**). Vertical error bars give uncertainty in δ^{18}O measurements (2σ) and horizontal error bars give decadal averages of age-model uncertainty in units of year/age-model year[10]. s.d. units, standard deviation units. **b,** Kiritimati coral δ^{18}O anomalies (‰ relative to the Pee Dee Belemnite (PDB) isotopic standard) and Sr/Ca anomalies (mmol mol^{-1}) relative to the mean for the 1981–87 period. Reproducibility confidence intervals (estimated 2σ) for each tracer are as indicated. Also plotted are estimates of SST anomalies from the analysis by Reynolds and Smith[14] for the 2°×2° grid box encompassing Kiritimati. The data have been plotted on a common range so that direct comparisons of the different measurements may be made: 8 °C ≈ 1.6‰ in δ^{18}O ≈ 0.6 mmol mol^{-1} in Sr/Ca[3,6]. **c,** Plot of NINO-C and NINO3 indices (SST anomalies averaged over 150°–90° W, 5° N to 5° S) against time. Also shown are the numbers of samples analysed per year and of SST observations per year. Correlation between NINO-C and NINO3 is −0.79.
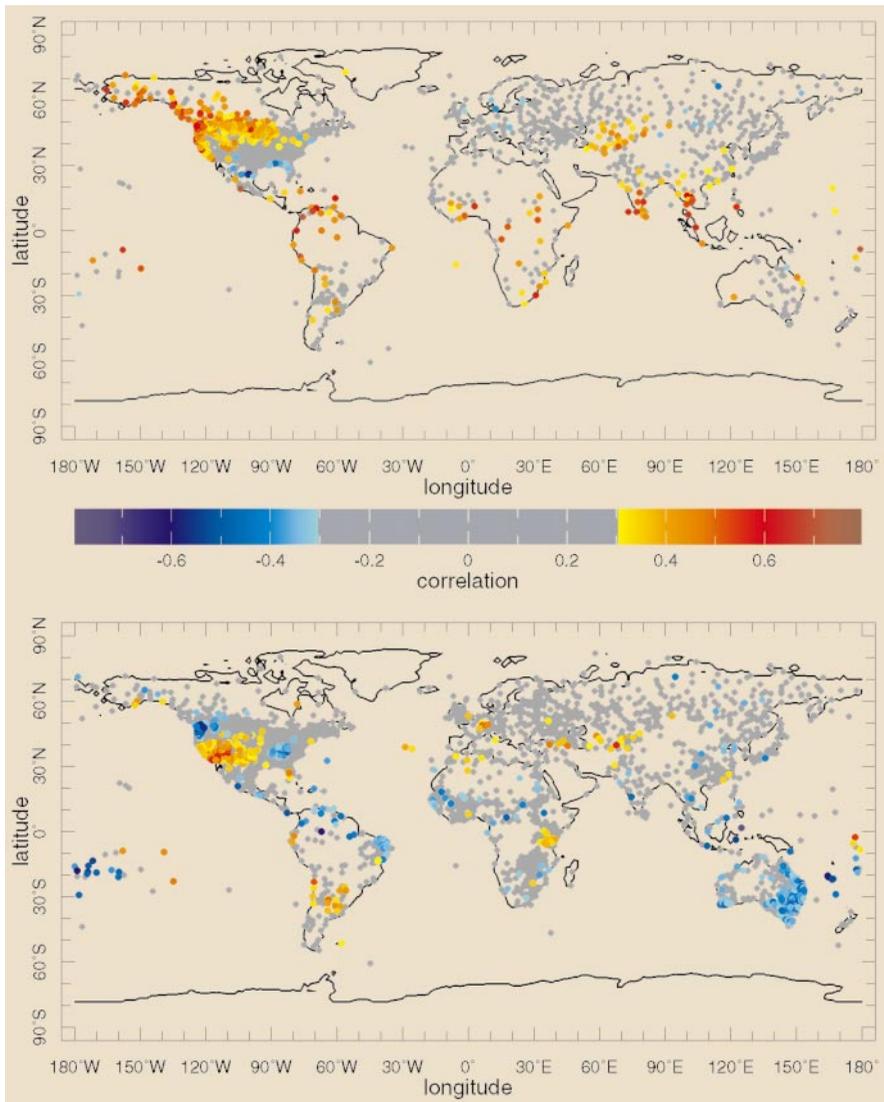
Figure 2 Linear correlations (*r*) between NINO-C and surface air temperature (top) or precipitation data (bottom) from a global network of stations[15]. The correlation maps have been multiplied by -1 so that positive (negative) correlations are associated with positive (negative) SST anomalies. The locations of all stations with $\leqslant 42$ years' worth of data are plotted in grey; stations correlated at or above the 90% confidence level ($|r| \geqslant 0.3$; ≈ 36 degrees of freedom) are plotted in colour. In general the recovered patterns agree with those recovered by correlation with like averages of NINO3, although there are subtle differences.

extratropical climate teleconnections[1,2,11–13]. However, correlations with NINO3 are stronger than correlations with NINO-C in the southeast United States for both temperature and precipitation, indicating that this region may be more sensitive to SST variability in the eastern than the central equatorial Pacific.

In contrast, surface temperatures in central and northeastern Asia at about 45° N appear to be responsive to NINO-C but not to NINO3. Thus there appear to be subtle differences between teleconnections associated with the central and eastern equatorial Pacific regions as well. These differences may be resolved by proxy indices from the central equatorial Pacific and other data-poor regions of the tropical oceans.

We have shown that NINO-C can provide a record of both tropical and extra-tropical climate variability on interannual time scales. Thus, comparison of modern and palaeoclimatic NINO-C results will allow analysis of climate change relative to the present, both in the central equatorial Pacific and in teleconnected regions. Seasonally variable carbon isotopic composition or density banding provides a relative chronology for a coral colony's lifetime, and absolute dating of fossil coral samples can be achieved by the radiocarbon or U-series techniques. By these means, multi-proxy extension of NINO-C into the pre-instrumental period will allow exploration of links to documented extratropical palaeoclimate anomalies on interdecadal time scales.

M. N. Evans*†, R. G. Fairbanks*†, J. L. Rubenstone*

**Lamont–Doherty Earth Observatory of Columbia University, Palisades, New York 10964-8000, USA*
†*Department of Earth and Environmental Sciences, Columbia University, New York, New York 10027, USA*
e-mail: mevans@ldeo.columbia.edu

1. Pan, Y. H. & Oort, A. H. *Mon. Weath. Rev.* **111,** 1244–1258 (1983).
2. Graham, N. E. & Barnett, T. P. *Science* **238,** 657–659 (1987).
3. Weber, J. N. & Woodhead, P. M. J. *J. Geophys. Res.* **77,** 463–473 (1972).
4. Cole, J. E., Fairbanks, R. G. & Shen, G. T. *Science* **260,** 1790–1793 (1993).
5. Weber, J. N. *Geochim. Cosmochim. Acta* **37,** 2173–2190 (1973).
6. DeVilliers, S., Shen, G. T. & Nelson, B. K. *Geochim. Cosmochim. Acta* **58,** 197–208 (1994).
7. McCulloch, M. T., Gagan, M. K., Mortimer, G. E., Chivas, A. R. & Isdale, P. J. *Geochim. Cosmochim. Acta* **58,** 2747–2754 (1994).
8. Philander, S. G. H. *El Niño, La Niña, and the Southern Oscillation* (Academic, San Diego, 1990).
9. Gagan, M. K., Chivas, A. R. & Isdale, P. J. *Geology* **24,** 1009–1012 (1996).
10. Evans, M. N. *et al. J. Geophys. Res.* (submitted); preprint available at <http://rainbow.ldeo.columbia.edu/~mevans/preprints/> (1998).
11. Ropelewski, C. F. & Halpert, M. S. *Mon. Weath. Rev.* **114,** 2352–2362 (1987).
12. Ropelewski, C. F. & Halpert, M. S. *J. Clim.* **2,** 268–284 (1989).
13. Halpert, M. S. & Ropelewski, C. F. *J. Clim.* **5,** 577–593 (1992).
14. Reynolds, R. W. & Smith, T. M. *J. Clim.* **7,** 929–948 (1994).
15. Baker, C. B. *et al.* in *Preprints of AMS Ninth Conf. Appl. Climatol., Dallas, 15–20 Jan. 1995*; also <http://ingrid.ldgo.columbia.edu/SOURCES/.NOAA/.NCDC/.GCPS/> (1998).

activity[9]. This sampling resolution allowed us to obtain 25–35 samples per annual band and to achieve a chronology with better-than-monthly resolution and low age-model error estimates[10] (Fig. 1a).

Paired $\delta^{18}O$ and Sr/Ca results and SST data for the 1981–86 period confirm that both geochemical thermometers captured the interannual SST variability over this six-year period, which includes the strong ENSO warm event of 1982–83, normal/cold conditions throughout mid-1986, and the initiation of the 1986–87 warm-phase event (Fig. 1b). As our interest here is in the inter-annual variability, we analysed further only April-to-March annual averages of the oxygen isotopic record, which we term 'NINO-C' and interpret as being primarily driven by SST anomalies (Fig. 1c). NINO-C shares over 60% variance with the commonly used NINO3 area index (150°–90° W, 5° N to 5° S) of the eastern equatorial Pacific SST anomaly[10].

NINO-C should also provide a good index of teleconnections associated with ENSO, as SST extremes in the central equatorial Pacific directly influence the atmospheric circulation[1,2]. Analysis of correlation patterns between data from surface meteorological stations and NINO-C indicates that global, interannual patterns of surface air temperature and precipitation anomalies are recoverable from NINO-C (Fig. 2) in the Americas, Africa, Australia, India and southeast Asia.

These patterns generally agree, in both spatial distribution and correlation amplitude, with those recovered by correlation of station data with like averages of NINO3 and with the literature on tropical–